Electronic Supplementary Material (ESI) for Lab on a Chip.

Electronic Supplementary Information

UV-visible spectroscopy of Silver nanoparticles (AgNPs)

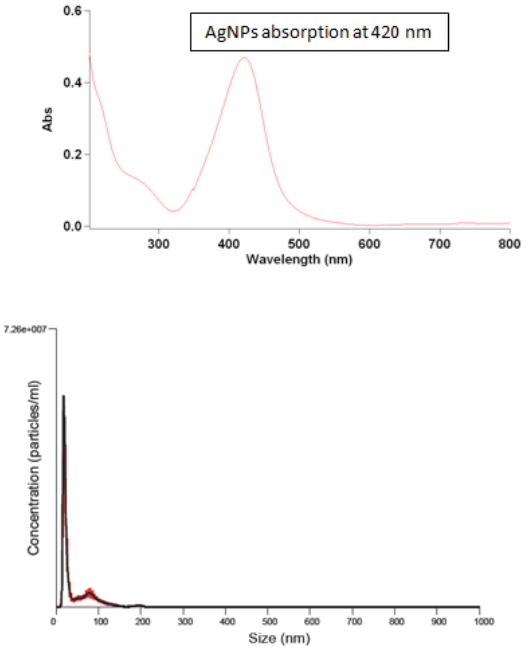

Fig. S1 Physico-chemical properties (UV-Visible, size) of AgNPs.

Distribution of a dye solution in three inlet straight channel

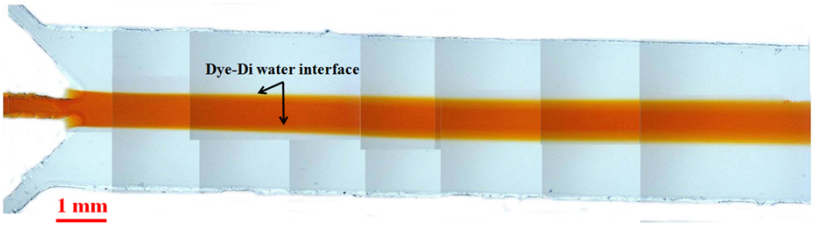

Fig. S2 The distribution of dye solution in a three inlet straight rectangular channel. In this superimposed image, individual microscopic images are captured along the alternate width and length of the microchannel to visualize the complete profile in full-length scale.

Hydrodynamic focusing in 30 nm fluorescent particles in three inlet straight channel

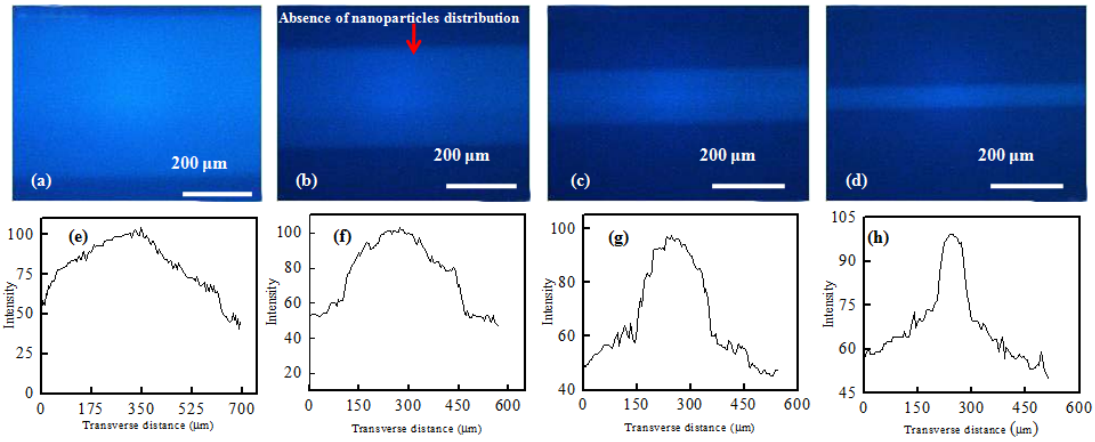

Fig. S3 Hydrodynamic focusing of fluorescent nanoparticles (30 nm) in straight rectangular microchannel. (a-d) Microscopic fluorescent images at 470 nm wavelength at different flow rate ratios of nanoparticles solution and DI water (25:25, 25:50, 25:100 and 25:250 respectively). (e-h) Plots of fluorescence intensity versus distance along the width of the channel showing a nearly parabolic profile for the 30 nm particles distributions instead of partial splitting of the central fluid as obtained in the converging-diverging channel.

Determination of reaction time by in-situ interaction of AgNPs and H_2O_2 in the converging-diverging microchannel

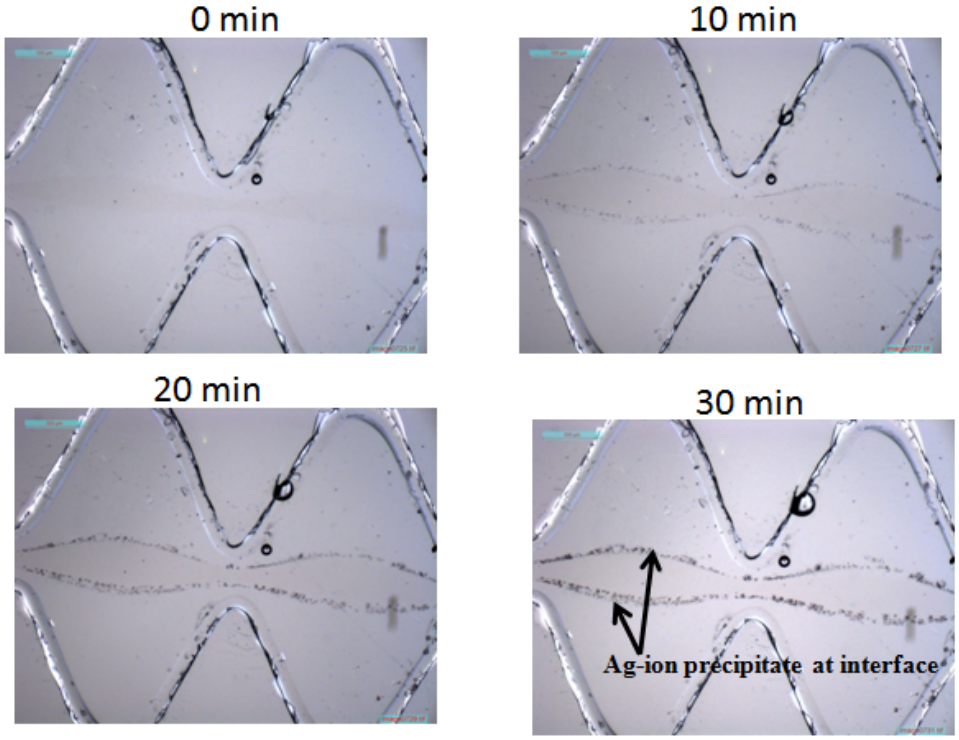

Fig. S4 Determination of the 30 min reaction time by performing the reaction between AgNPs and H_2O_2 at different time intervals.

Confirmation of Ag ion precipitate as flowing aqueous NH_3 through the channel containing Ag ion precipitate.

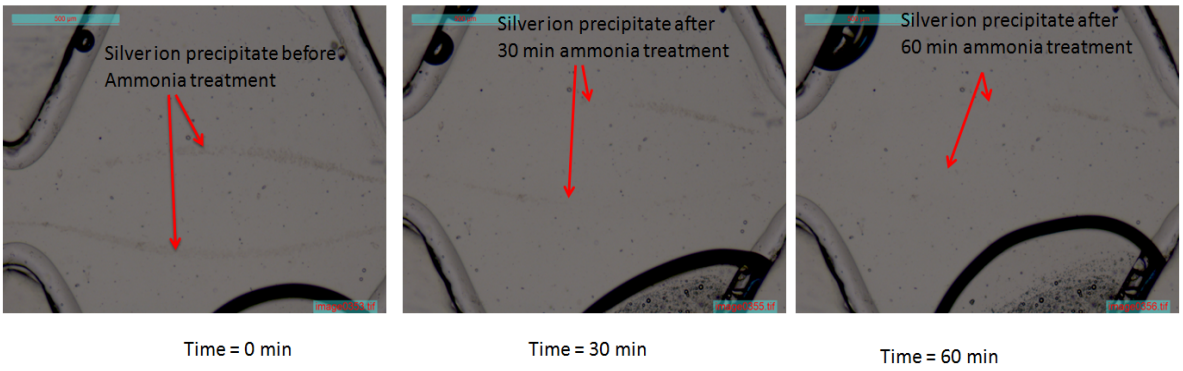

Fig. S5 Confirmation of the silver ion precipitate as a product by introducing aqueous NH_3 in channel. Arrows indicate the silver ion precipitates which disappear with time due to the formation of the diamminesilver ion ($[Ag(NH_3)_2]^+$).

Numerical simulation details in the converging-diverging channel

For our simulation purpose, we solve the full Navier-Stokes equation, along with the incompressibility criterion, to obtain the velocity field of the carrier phase. We consider the density and dynamic viscosity of the carrier phase as 1000 kg/m^3 and 0.001003 kg/m-s, respectively. These considerations are in accordance with the thermo-physical properties of the aqueous medium, used for the present experimental purpose. The particle dynamics is captured through the consideration of the forces and interactions, as detailed in the main paper. In Fig. S6 we demonstrate the present simulation domain. All the simulations are conducted with respect to a fixed-to-the-lab Cartesian reference frame, as shown in Fig. S6. Primarily, the flow is imposed along the x direction. We consider no-slip, no-penetration boundary conditions over the solid walls of the channel. Owing to the periodically repeated geometry of the channel, we consider periodic boundary condition along the x direction. With the above mentioned considerations in background, we solve the transport equations following the finite volume method invoking pressure-velocity coupling through SIMPLE algorithm (Patankar 1980), in a fully time-implicit framework, using the platform of FLUENT®. The simulations are performed using uniform grids, as represented in Fig. S1. We conduct simulations with resolutions of 1 mm, 0.05 mm, 0.02 mm and 0.01 mm. Taking numerical accuracy and computational expenses in combined consideration, it is observed that grid size of 0.02 mm provides the optimum performance, and is used for the simulation study.

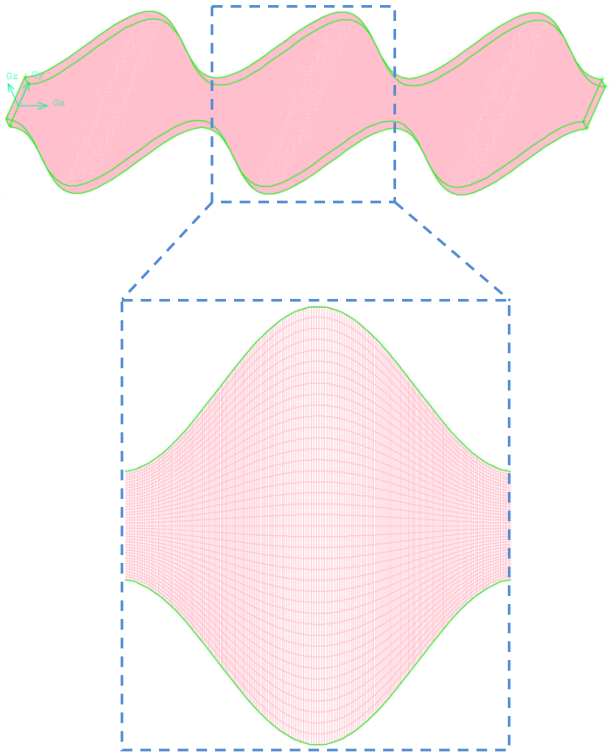

Fig. S6 Description of the present simulation domain. The magnified portion highlights the domain discretization with uniform grids.